Supporting Information

Gonzalez et al. 10.1073/pnas.1307525111

SI Materials and Methods

Yeast Growth Media. Standard synthetic media were used: yeast extract-peptone-dextrose (YPD) contained 2% (wt/vol) glucose and complete synthetic media contained 0.6% casamino acids and/or individual amino acid supplements.

Ubiquitination Assays. In all experiments, cells were treated with 1% formaldehyde for 2 min to trap ubiquitinated intermediates. Cross-linking was quenched, and extracts were made in immunoprecipitation buffer (50 mM Tris·HCl, pH 8.0, 150 mM NaCl, 5 mM EDTA, 1% Triton-X 100, 1 mM DTT, and protease inhibitor mixture II; Calbiochem). Extracts (100 μg) were precleared with protein G magnetic beads (Qiagen) for 1 h at room temperature. Anti-HA (10 μg; Santa Cruz Biotechnology) was added, and samples were incubated at 4 °C overnight. Fifty microliters of protein G magnetic beads was added, and samples were incubated on ice for 2 h. Immobilized proteins were washed three times in immunoprecipitation buffer and eluted, and cross-links were reversed in SDS sample buffer. Proteins were separated by SDS/PAGE, transferred to membranes, and probed with rabbit anti-ubiquitin (donated by S. Reed, Cardiff University, Cardiff, UK) or anti-HA antibody.

LC and MS. Tap-purified proteins were reduced with 6.5 mM DTT in 50 mM ammonium bicarbonate, alkylated with 54 mM iodoacetamide in 50 mM ammonium bicarbonate, and digested with trypsin (Promega). Combined digests of ^{14}N- and ^{15}N-labeled samples were subjected to strong cation exchange (SCX) chromatography followed by automated on-line sandwich reverse phase (RP)-TiO_2-RP LC-MS/MS to enrich for phosphopeptides as described elsewhere (1). Briefly, collected fractions were analyzed by nanoflow LC using an Agilent 1100 HPLC system (Agilent Technologies) coupled on-line to a LTQ-Orbitrap mass spectrometer (ThermoFisher Scientific). Phosphopeptides were trapped and enriched on three separate precolumns [two 3-cm × 100-μm inner diameter Aqua C_{18} (Phenomenex) and a 5-cm × 100-μm inner diameter TiO_2 (GL Sciences), all packed in house] and separated on a 20-cm analytical column [ReproSil-Pur C_{18}-AQ 3-μm; (Dr. Maisch GmbH), 50-μm inner diameter, packed in house] at ∼100 nL/min in a 60-min gradient from 10% to 40% solvent [0.1 M acetic and 0.13 M formic acid in 8:2 (vol/vol) acetonitrile/water]. The eluent was sprayed via standard coated emitter tips (New Objective) into an LTQ-Orbitrap, which was operated in data-dependent mode, automatically switching between MS, MS/MS, and neutral loss driven MS^3. Full-scan MS spectra (m/z 400–1,500) were acquired with a resolution of 60,000 (at m/z 400), and the two most intense ions were selected for MS/MS fragmentation in the linear ion trap. Raw data were converted to DTA files using Bioworks 3.2 and merged into Mascot Generic Format files, which were searched against the Saccharomyces Genome Database (SGD) using Mascot (version 2.2) as a search engine. Carbamidomethylation of cysteine was set as fixed modification; methionine oxidation and serine, threonine, and tyrosine phosphorylation were set as variable modifications, selecting ^{15}N labeling as quantification mode. The mass tolerance of the precursor ion was 10 ppm and 0.9 Da for fragment ions. The false discovery rate was set at <1% (Mascot score threshold of 35) using the decoy database approach. MSQuant (2) was used for peptide quantification; localization of phosphorylation sites was determined in Mascot version 2.4.

1. Lemeer S, et al. (2008) Comparative phosphoproteomics of zebrafish Fyn/Yes morpholino knockdown embryos. *Mol Cell Proteomics* 7(11):2176–2187.

2. Gouw JW, Krijgsveld J (2012) MSQuant: A platform for stable isotope-based quantitative proteomics. *Methods Mol Biol* 893:511–522.

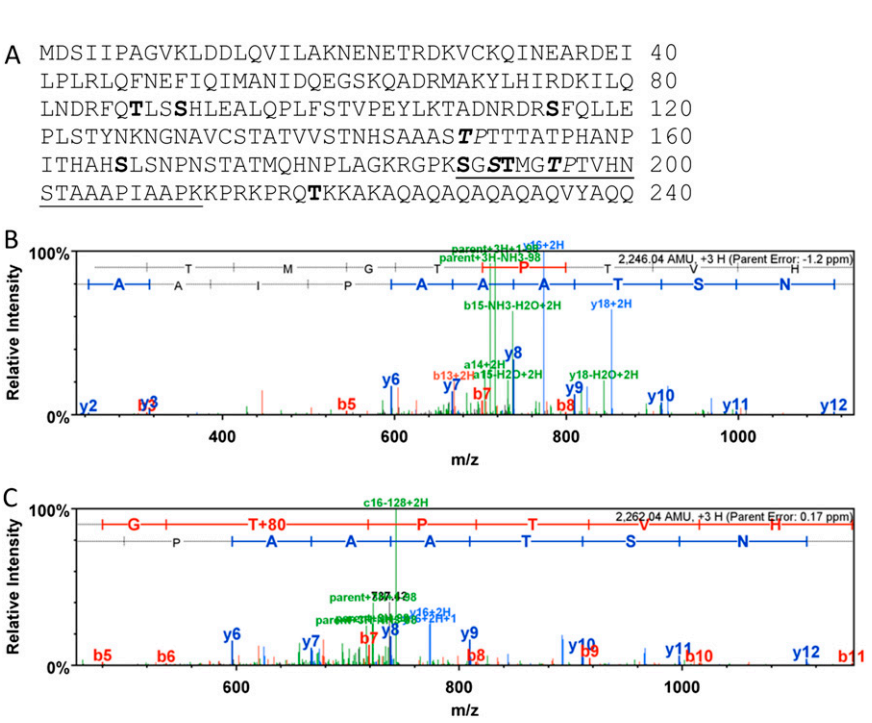

Fig. S1. NetPhos prediction and mass spectra for Med3phosphorylation sites. (*A*) Predicted Cdk8 phosphorylation sites in Med3. The predicted peptide sequence of Med3ΔSal1 (amino acids 1–234) was analyzed using Netphos 2 (1). All predicted serine and threonine phosphorylation sites with significant Netphos scores are shown (S/T, bold). The single Med3 phospho-peptide detected by tandem mass spectrometry (MS/MS) (underlined) contains one of the two predicted Cdk8 phosphorylation sites (T195P, italicized), and a second phosphorylation site (S191, italicized) detected by LC-MS/MS are shown. (*B*) MS/MS spectrum of SGSTMGT(phos)PTVHNSTAAAPIAAPK. (*C*) MS/MS spectrum of SGS(phos)TMGTPTVHNSTAAAPIAAPK.

1. Blom N, Gammeltoft S, Brunak S (1999) Sequence and structure-based prediction of eukaryotic protein phosphorylation sites. *J Mol Biol* 294(5):1351–1362.

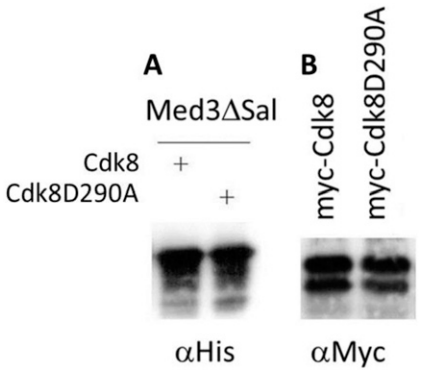

Fig. S2. In vitro phosphorylation of Med3 by purified Cdk8. (*A*) Med3ΔSal input protein detected using anti-histidine tag antibody. (*B*) myc-epitope tagged Cdk8 purified from yeast cells grown by immunoprecipitation using anti-myc antibody.

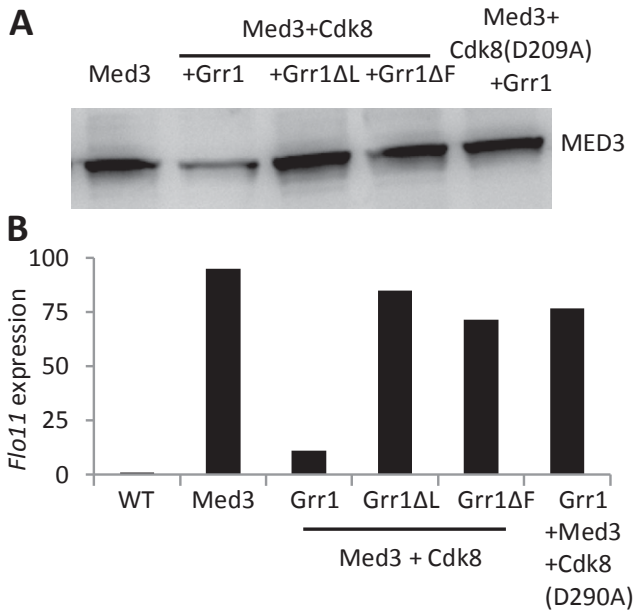

Fig. S3. Interaction of Med3 and Grr1 regulates *FLO11* expression. (*A*) Stability of ectopically expressed Med3 is decreased by Grr1 and Cdk8. HA-Med3 was immunoprecipitated from cells expressing MED3, GRR1, and nonfunctional Grr1ΔL or Grr1ΔF derivatives, together with CDK8 (GIG-2) or the kinase inactive variant (*cdk8*D290A, GIG-3). Following separation and blotting, membranes were probed with anti-HA antibody. (*B*) Cells were transformed with *MED3*, *CDK8*, or *cdk8* (D290A) and *GRR1* (where indicated). Total RNA was isolated and *FLO11* expression levels determined using quantitative RT-PCR analysis. Flo11 relative starting quantities were normalized to *ACT1* and values are given as percentage relative to WT.

Table S1. Med3 interacts with Cdk8 in vivo

	Med3	Med3ΔSal	Ssn6	pACT2
Fold activation	5.2	2.7	2.8	1

In vivo interaction between full-length and the N-terminal region of Med3 (Med3ΔSal) and Cdk8. Yeast was transformed with LexA-Cdk8 as bait, the indicated prey plasmids, and a LacZ reporter gene (JK103), and β-galactosidase levels were determined for at least five independent transformants. Ssn6 is a positive control. Fold increase in reporter gene activation over negative control (pACT2) is given.

Table S2. List of genes that change at least 1.7-fold in any single deletion mutant grr1Δ

Systematic name	Standard name	Name
Block I		
YBL078C	ATG8	Autophagy related
YBR072W	HSP26	Heat shock protein
YBR169C	SSE2	
YBR285W		
YER035W	EDC2	Enhancer of mRNA decapping
YER053C	PIC2	PI carrier
YHR138C		
YIL107C	PFK26	6-phosphofructo-2-kinase
YKL103C	APE1	Aminopeptidase
YKL133C		
YFR017C	IGD1	Inhibitor of glycogen debranching
YDL085W	NDE2	NADH dehydrogenase, external
YDL110C	TMA17	Translation machinery associated
YGL121C	GPG1	G protein gamma
YGL156W	AMS1	Alpha-mannosidase
YGR070W	ROM1	Rho1 multicopy suppressor
YJL141C	YAK1	However, another kinase
YJL142C	IRC9	Increased recombination centers
YJL163C		
YJL199C	MBB1	
YLL026W	HSP104	Heat shock protein
YLR178C	TFS1	cdc25 suppressor
YLR270W	DCS1	Decapping scavenger
YLR356W	ATG33	Autophagy related
YLR400W		
YMR174C	PAI3	Proteinase A inhibitor
YMR175W	SIP18	Salt induced protein
YMR196W		
YNL115C		
YNL200C		
YOL083W	ATG34	Autophagy related
YOR289W		
YPL123C	RNY1	Ribonuclease from yeast
YPL230W	USV1	Up in starvation
YPR151C	SUE1	
Block II		
YAL017W	PSK1	Pas domain-containing serine/threonine protein kinase
YAL061W	BDH2	
YBR001C	NTH2	Neutral trehalase
YBR026C	ETR1	2-enoyl thioester reductase
YBR046C	ZTA1	Zeta-crystallin
YBR067C	TIP1	Temperature shock-inducible protein
YBR105C	VID24	Vacuolar import and degradation
YBR132C	AGP2	High-affinity glutamine permease
YBR149W	ARA1	D-Arabinose dehydrogenase
YCL042W		
YCR004C	YCP4	
YCR011C	ADP1	ATP-dependent permease
YCR091W	KIN82	protein kinase
YEL011W	GLC3	Glycogen
YEL060C	PRB1	Proteinase B
YER079W		
YER098W	UBP9	Ubiquitin-specific protease
YER141W	COX15	Cytochrome c oxidase
YHL021C	AIM17	Altered inheritance rate of mitochondria
YHR008C	SOD2	Superoxide dismutase
YHR054C		
YHR080C		
YHR096C	HXT5	Hexose transporter
YIL055C		
YIL136W	OM45	Outer membrane 45 protein
YIL155C	GUT2	Glycerol utilization 2 protein

Table S2. Cont.

Systematic name	Standard name	Name
YIL160C	POT1	Peroxisomal oxoacyl thiolase
YIR019C	FLO11	Flocculation protein
YKL091C		
YKL093W	MBR1	Mitochondrial biogenesis regulation
YKL142W	MRP8	Mitochondrial ribosomal protein
YKL150W	MCR1	Mitochondrial NADH-cytochrome b5 reductase
YKL187C	FAT3	Fatty acid transporter 3
YKR039W	GAP1	General amino acid permease
YFL036W	RPO41	RNA polymerase
YDL049C	KNH1	Kre9 (nine) homolog
YDL169C	UGX2	Unidentified gene X2
YDL181W	INH1	Inhibitor ATPase
YDL199C		
YDR032C	PST2	Protoplasts-secreted
YDR096W	GIS1	GIg1-2 suppressor
YDR100W	TVP15	Tlg2-vesicle protein
YDR133C		
YDR216W	ADR1	Alcohol dehydrogenase regulator
YDR231C	COX20	Cytochrome c oxidase
YDR343C	HXT6	Hexose transporter
YDR504C	SPG3	Stationary phase gene
YDR505C	PSP1	Polymerase suppressor
YGL006W	PMC1	Plasma membrane calcium
YGL037C	PNC1	Pyrazinamidase and nicotinamidase
YGL205W	POX1	
YGL227W	VID30	Vacuolar import and degradation
YGR008C	STF2	Stabilizing factor
YGR023W	MTL1	Mid-two like 1
YGR110W	CLD1	Cardiolipin-specific deacylase
YGR130C		
YGR174C	CBP4	Cytochrome B mRNA processing
YGR192C	TDH3	Triose-phosphate dehydrogenase
YGR249W	MGA1	
YGR279C	SCW4	Soluble cell wall protein
YJL048C	UBX6	Ubiquitin regulatory X
YJL066C	MPM1	Mitochondrial peculiar membrane protein
YJL079C	PRY1	Pathogen related in yeast
YJL088W	ARG3	Arginine requiring
YJL164C	TPK1	Takashi's protein kinase
YJL185C	ATG36	Autophagy related
YJR008W	MHO1	Memo homolog
YLL019C	KNS1	Kinase next to SPA2
YLL020C		
YLR042C		
YLR120C	YPS1	Yapsin
YLR149C		
YLR258W	GSY2	Glycogen synthase
YLR345W		
YLR375W	STP3	Protein with similarity to Stp1p
YML054C	CYB2	Cytochrome B
YML128C	MSC1	Meiotic sister-chromatid recombination
YMR031C	EIS1	Eisosome
YMR105C	PGM2	Phosphoglucomutase
YMR107W	SPG4	Stationary-phase gene
YMR136W	GAT2	
YMR145C	NDE1	NADH dehydrogenase, external
YMR173W	DDR48	DNA damage responsive
YMR199W	CLN1	Cyclin 1
YMR251W-A	HOR7	Hyperosmolarity-responsive
YMR297W	PRC1	Proteinase C
YNL015W	PBI2	Proteinase B inhibitor
YNL031C	HHT2	Histone H three

Table S2. Cont.

Systematic name	Standard name	Name
YNL055C	POR1	Porin
YNL100W	AIM37	Altered inheritance rate of mitochondria
YNL180C	RHO5	Ras homolog
YNL194C		
YNL195C		
YNL237W	YTP1	Yeast putative transmembrane protein
YNL274C	GOR1	Glyoxylate reductase
YNL289W	PCL1	Pho85 cyclin
YNL305C	BXI1	Bax inhibitor
YOL011W	PLB3	Phospholipase B
YOL058W	ARG1	Arginine requiring
YOL081W	IRA2	Inhibitory regulator of the RAS-cAMP pathway
YOL084W	PHM7	Phosphate metabolism
YOR173W	DCS2	Decapping scavenger
YOR178C	GAC1	Glycogen accumulation
YOR215C	AIM41	Altered inheritance of mitochondria
YOR302W		
YOR317W	FAA1	Fatty acid activation
YOR348C	PUT4	Proline utilization
YOR374W	ALD4	Aldehyde dehydrogenase
YPL004C	LSP1	Long chain bases stimulate phosphorylation
YPL024W	RMI1	RecQ mediated genome instability
YPL026C	SKS1	Suppressor kinase of SNF3
YPL087W	YDC1	Yeast dihydroceramidase
YPL154C	PEP4	Carboxypeptidase Y-deficient
YPL186C	UIP4	Ulp1 interacting protein
YPL222W	FMP40	Found in mitochondrial proteome
YPR026W	ATH1	Acid trehalase
YPR065W	ROX1	Regulation by oxygen
YPR098C		
YPR149W	NCE102	Nonclassical export
YPR184W	GDB1	
YDL130W-A	STF1	Stabilizing factor
YGR161C-D		
YDR261W-B		
YBR085C-A		
YNR034W-A		

cdk8Δ vs. WT, $P \leq 0.05$.

Table S3. Yeast strains used in this study

Strain	Relevant genotype	Reference
FT5	*MATα; ura3-52; trp1Δ65; his3Δ200; leu2::PET56*	(1)
L9FT5	*MATα; ura3-52; trp1Δ65; his3Δ200; leu2::PET56*; 4XLexA Operator-TATA-His3	(2)
Z718	*MATα; ura3-52; his3Δ200; leu2-3*	(3)
Cdk8Δ	*MATα; ura3-52; his3Δ200; leu2-3*	(3)
Cdk8Δ med3ΔHIS3	*MATα; ura3-52; leu2-3*	This study
Cdk8Δ med2ΔHIS3	*MATα; ura3-52; leu2-3*	This study
Cdk8Δ spt8ΔKanR	*MATα; ura3-52; his3Δ200; leu2-3; YLR055c::kanMX4*	This study
Cdk8ΔD290A	*MATα; ura3-52; his3Δ200; leu2-3*	(3)
Cdk8ΔD290A med3ΔHIS3	*MATα; ura3-52; leu2-3*	This study
med3ΔHIS3	*MATα; ura3-52; leu2-3*	This study
med2ΔHIS3	*MATα; ura3-52; leu2-3*	This study
spt8Δ KanR	*MATα; ura3-52; his3Δ200; leu2-3; YLR055c::kanMX4*	This study
JN 284 (Ise1)	*MATα his7 leu2 ura3 ise1*	(4)
BY4741	*MATα; his3Δ1; leu2Δ0; met15Δ0; ura3Δ0*	EUROSCARF (5)
grr1Δ	*MATa; his3Δ1; leu2Δ0; met15Δ0; ura3Δ0; YJR090c::kanMX4*	EUROSCARF (5)
Med3-TAP	*MATα ade2 arg4 leu2-3,112 trp1-289 ura3-52*	EUROSCARF (6)
Med3 -TAPgrr1Δ	TAP-tagged strain *MED3 grr1Δ*	This study
Med15-TAP	YPH499, YDL005c:TAP-K.l.TRP1	This study
Med15-TAP cdk8Δ	YPH499, YDL005c:TAP-K.l.TRP1	This study
YC7	*MAT* **a** *his3Δ200 leu2-3,112 ura3-52 srb10-3^{myc9}::hisG*	(7)
YC17	*MAT* **a** *his3Δ200 leu2-3,112 ura3-52 SRB10^{myc9}*	(7)

1. Tzamarias D, Struhl K (1994) Functional dissection of the yeast Cyc8-Tup1 transcriptional co-repressor complex. *Nature* 369(6483):758–761.
2. Tzamarias D, Struhl K (1995) Distinct TPR motifs of Cyc8 are involved in recruiting the Cyc8-Tup1 corepressor complex to differentially regulated promoters. *Genes Dev* 9(7):821–831.
3. Liao SM, et al. (1995) A kinase-cyclin pair in the RNA polymerase II holoenzyme. *Nature* 374(6518):193–196.
4. Lee DH, Goldberg AL (1996) Selective inhibitors of the proteasome-dependent and vacuolar pathways of protein degradation in Saccharomyces cerevisiae. *J Biol Chem* 271(44): 27280–27284.
5. Brachmann CB, et al. (1998) Designer deletion strains derived from Saccharomyces cerevisiae S288C: A useful set of strains and plasmids for PCR-mediated gene disruption and other applications. *Yeast* 14(2):115–132.
6. Gavin AC, et al. (2006) Proteome survey reveals modularity of the yeast cell machinery. *Nature* 440(7084):631–636.
7. Chi Y, et al. (2001) Negative regulation of Gcn4 and Msn2 transcription factors by Srb10 cyclin-dependent kinase. *Genes Dev* 15(9):1078–1092.

Table S4. Plasmids used in this study

Plasmid	Relevant characteristics	Source
e2p6-HRS1	2-μm plasmid, MED3 over-expressed, ADH1 promoter	(1)
e2p6-HRS1T195A	2-μm plasmid, MED3T195A over-expressed, ADH1 promoter	This study
e2p6-HRS1S191G	2-μm plasmid, MED3S191G over-expressed, ADH1 promoter	This study
e2p6-MED2	2-μm plasmid, MED2 over-expressed, ADH1 promoter	(1)
pGIG2	2-μm plasmid, CDK8 over-expressed, Own promoter intact	(2)
pGIG2-3	2-μm plasmid, CDK8D290A over-expression, Own promoter intact	This study
pRS403	Yeast Integrating plasmid, ampicillin resistance, HIS3 selection	(3)
pRS405	Yeast Integrating plasmid, ampicillin resistance, LEU2 selection	(3)
BM2961	2-μm plasmid, LexA-grr1	(4)
pRSTMED3	(6xHis) tagMED3, inducible T7 promoter	(1)
pRSTMED3ΔSal	(6xHis) tagMED3 ΔSal, inducible T7 promoter	This study
pRW0123081	pAS2-GRR1	(5)
pRW040981	pAS2-GRR1ΔL	(5)
pRW0411081	pAS2-GRR1ΔF	(5)
BM3383	pT7-Grr1ΔN	(4)

1. Papamichos-Chronakis M, Conlan RS, Gounalaki N, Copf T, Tzamarias D (2000) Hrs1/Med3 is a Cyc8-Tup1 corepressor target in the RNA polymerase II holoenzyme. *J Biol Chem* 275(12): 8397–8403.
2. Balciunas D, Ronne H (1995) Three subunits of the RNA polymerase II mediator complex are involved in glucose repression. *Nucleic Acids Res* 23(21):4421–4425.
3. Sikorski RS, Hieter P (1989) A system of shuttle vectors and yeast host strains designed for efficient manipulation of DNA in Saccharomyces cerevisiae. *Genetics* 122(1):19–27.
4. Li FN, Johnston M (1997) Grr1 of Saccharomyces cerevisiae is connected to the ubiquitin proteolysis machinery through Skp1: Coupling glucose sensing to gene expression and the cell cycle. *EMBO J* 16(18):5629–5638.
5. Wang R, Solomon MJ (2012) Identification of She3 as an SCF(Grr1) substrate in budding yeast. *PLoS ONE* 7(10):e48020.

Table S5. Primers used in this study

Primers	Sequence 5′ to 3′
ACT1-ORF-f	TCCCAGGTATTGCCGAAAGAATG
ACT1-ORF-r	AGCCAAGATAGAACCACCAATCC
FLO11-ORF-f	GTATGCTCTGCTAAGACTATCG
FLO11-ORF-r	GCCAGCGGAGTTAGTACC
FLO11-HSL-f	AAAGCAACTATTAGGGTACGATTG
FLO11-HSL-r	AAAAGAACGAAGTATATTGCGATG
FLO11-TATA-f	ACGGATAACTCATAGACTTACCAG
FLO11-TATA-r	CACAACATGACGAGGGATAATAAC
GIG2mut-f	CCATAGATGGATGTGTTAAAATTGGTGCTTTAGGTTTGGCCAG
GIG2mut-r	CTGGCCAAACCTAAAGCACCAATTTTAACACATCCATCTATGG
MED2HIS3-f	CGGATCCTCCCAAATAAACTGCCCGTCTGAAAGTA GGAGTCACTGCCAGGTATCG
MED2HIS3-r	TTTACAAGTCAATAGTTAACAATAGGAAGACCAAG CGCCTCGTTCAGAATGACAC
SRB10HIS3-f	TTAAGGCCGCCTAGTTTTGACGGGAGGAGAGAGAAGGAGTCACTGCCAGGTATCG
SRB10HIS3-r	CTATCTTCTGTTTTTCTTTCGAGATGGCTCATCTGCGCCTCGTTCAGAATGACAC
GRR1LEU-f	GCCGCCTAGT TTTGACGGGA GGAGAGAGAA CTGTGCGGTATTTCACACCG
GRR1LEU-r	GCTGTGGAAT GAAAAATTCC AAATATATAT AAAAATAGAA GCC AGATTGTACTGAGAGTGCAC
SPT8HIS3-f	CGTAATGGACGAGGTTGACGATATTCTAATTAACAGGAGTCACTGCCAGGTATCG
SPT8HIS3-r	GTCTATATCGTAAATAAGGGTCGTGTCCGTAGAATCGCCTCGTTCAGAATGACAC

Dataset S1. Peak lists generated from raw MS data and subsequent database search results from peak lists input

Dataset S1